



Removal of methylene blue from aqueous solution using chitosan-g-poly (acrylic acid)/montmorillonite superadsorbent nanocomposite

Li Wang^{a,b,c}, Junping Zhang^{a,b}, Ai Qin Wang^{a,*}

^a Center of Eco-material and Green Chemistry, Lanzhou Institute of Chemical Physics, Chinese Academy of Sciences, Lanzhou 730000, PR China

^b Graduate School of the Chinese Academy of Sciences, Beijing 100049, PR China

^c College of Forestry Engineering, Inner Mongolia Agricultural University, Hohhot 010018, PR China

ARTICLE INFO

Article history:

Received 11 October 2007

Received in revised form 5 January 2008

Accepted 19 February 2008

Available online 26 February 2008

Keywords:

Superadsorbent nanocomposite

Montmorillonite

Chitosan

Adsorption

Methylene blue

ABSTRACT

Batch adsorption experiments were carried out for the removal of methylene blue (MB) cationic dye from its aqueous solution using chitosan-g-poly(acrylic acid)/montmorillonite (CTS-g-PAA/MMT) nanocomposites as adsorbent. The factors influencing adsorption capacity of the nanocomposite such as initial pH value (pH_0) of the dye solution, MMT content (wt%), weight ratio (wr) of AA to CTS and adsorption temperature (T) were investigated. The results showed that the wr of AA to CTS of the nanocomposites have great influence on adsorption capacities and introducing a small amount of MMT could improve adsorption ability of the CTS-g-PAA. The adsorption behaviors of the nanocomposite showed that the adsorption kinetics and isotherms were in good agreement with pseudo-second-order equation and the Langmuir equation, respectively, and the maximum adsorption capacity is 1859 mg/g for CTS-g-PAA/MMT with wt% of 30% and wr of 7.2:1. The desorption studies revealed that the nanocomposite provided the potential for regeneration and reuse after MB dye adsorption.

© 2008 Elsevier B.V. All rights reserved.

1. Introduction

Colored organic effluent is produced in industries such as textiles, rubber, paper, plastic, cosmetics, etc. [1]. The colored effluents of waste water from these industries can be mixed in surface water and ground water systems, and then they may also transfer to drinking water and bring a chief threat to human health due to either toxic or mutagenic and carcinogenic for most of dyes [2]. Therefore, colored wastewater cannot be discharged without adequate treatment. As dyes are designed to resist breakdown with time and exposure to sunlight, water, soap and oxidizing agent, they cannot be easily removed by conventional wastewater treatment processes due to their complex structure and synthetic origins [3]. Thus, dye removal has been an important but challenging area of wastewater treatment.

Among many methods for removing dyes include coagulation and flocculation [4], membrane separation [5], oxidation or ozonation [6,7], electro-coagulation [8] and adsorption [9], the adsorption is now an effective and economical method for the removal of dyes from waste water. It has been reported that many different types of adsorbents are effective in removing color from aqueous effluent. Recently, particular attention has been paid to polysaccharide and

clay-based adsorbents. The polysaccharide materials are gaining interest for application as adsorbents in wastewater treatment due to their biodegradable and non-toxic nature [10]. Chitosan (CTS) is the *N*-deacetylated derivative of chitin and the second most plentiful natural biopolymer. As a well-known sorbent, CTS is widely used for the removal of heavy, transition metals and dyes [11–13]. Nevertheless, CTS adsorb the cationic dyes in very small amounts because it is a natural cation polysaccharide. Moreover, the weak mechanical property and low specific gravity should be improved for practical operation.

Among many kinds of clay minerals, montmorillonite (MMT) has often been used in the removal of organic pigments and dyes [14–18] due to its low cost, high surface area and high-cation exchange capacity. In recent 20 years, many reports showed that MMT displayed comparatively high-adsorption capacity for methylene blue (MB) [19–21]. However, the expandability and dispersive suspendability of MMT in aqueous solution should be improved for practical operation. Therefore, several attempts have been made to develop more effective adsorbents.

Superadsorbents are three-dimensional polymeric networks whose main feature is the ability to absorb and retain water. The porous structure networks allow dye molecules diffusion through the superadsorbent. As a rule, the superadsorbent possess anion functional groups, they can absorb and trap cationic dyes, such as MB [22], from wastewaters. Thus, the superadsorbent may be used as an alternative adsorbent for the removal of cationic dyes

* Corresponding author. Tel.: +86 931 4968118; fax: +86 931 8277088.
E-mail address: aqwang@lzb.ac.cn (A. Wang).

from aqueous solution. However, to our best knowledge, there is no literature focusing on the adsorption capacity of cationic dye onto the superadsorbent based on polysaccharides and clays. So, on the basis of our previous work about the preparation and water absorbency of chitosan-g-poly(acrylic acid)/montmorillonite (CTS-g-PAA/MMT) nanocomposites [23], the adsorption capacities of the nanocomposites for MB were studied in this paper. The effects of pH value of the dye solution and adsorption temperature on the adsorption capacity of MB on the superadsorbent nanocomposite have been investigated. The adsorption kinetics and isotherms for MB dye onto CTS-g-PAA/MMT were also studied, and the desorption studies of the nanocomposite was discussed.

2. Experimental

2.1. Chemicals and materials

Acrylic acid (AA, distilled under reduced pressure before use), ammonium persulfate (APS, recrystallized from distilled water before use) and *N,N'*-methylenebisacrylamide (MBA, used as received) were supplied by Shanghai Reagent Corp. (Shanghai, China). The degree of deacetylation and a viscosity-average molecular weight of CTS (Zhejiang Yuhuan Ocean Biology Co., China) is 85% and 9.0×10^5 , respectively. The cationic exchange capacity (CEC) of MMT (Shandong Longfeng Montmorillonite Co., China) is 102.8 mequiv./100 g. MMT was ground and sieved to 320-mesh size. The molecular formula of MB (Shanghai Reagent Corp., China) is $C_{16}H_{18}N_3S$ and the molecular structure is shown in Fig. 1. Other agents used were all analytical grade and all solutions were prepared with distilled water.

2.2. Preparation of CTS-g-PAA/MMT nanocomposites and their characterization

A series of CTS-g-PAA/MMT nanocomposites from CTS, AA and MMT was prepared according to our previous reports using the one-step method via in situ intercalated polymerization [23]. The schematic process for synthesis of CTS-g-PAA/MMT nanocomposite is shown in Fig. 2. The preparation procedure of CTS-g-PAA is similar to that of the superadsorbent nanocomposites except without MMT. The product was milled and all samples used for test had a particle size of 200 mesh.

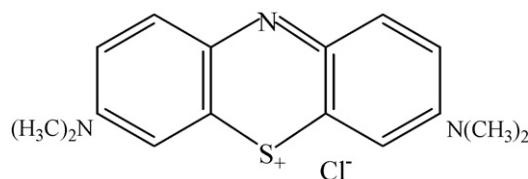


Fig. 1. The structure of MB.

IR spectra were taken as KBr pellets using a Thermo Nicolet NEXUS TM spectrophotometer. The absorption bands variety of IR spectra of MMT, CTS, CTS-g-PAA and CTS-g-PAA/MMT showed that graft reaction has taken place among CTS, AA and MMT. Power XRD analyzes were performed using an X-ray power diffractometer with Cu anode (PANalytical Co. X'pert PRO), running at 40 kV and 30 mA, scanning from 4° to 18° at $3^\circ/\text{min}$. After polymerization of the CTS-modified-MMT with AA, the typical diffraction peak of MMT cannot be detected no matter how much CTS-modified-MMT was introduced. This results showed that the CTS-modified-MMT with AA may form nanocomposite with intercalate-exfoliated nanostructure [23].

The point of zero charge (pH_{PZC}) of the CTS-g-PAA/MMT was determined by the solid addition method [24]. To a series of 100-mL conical flasks 45 mL of KNO_3 solution of known strength was transferred. The pH_0 values of the solution were roughly adjusted from 2 to 12 by adding either 0.1 mol/L HNO_3 or NaOH . The total volume of the solution in each flask was made exactly to 50 mL by adding the KNO_3 solution of the same strength. The pH of the solutions was then accurately noted, and 0.1 g of CTS-g-PAA/MMT was added to each flask, which were securely capped immediately. The suspensions were then manually shaken and allowed to equilibrate for 48 h with intermittent manual shaking. The pH values of the supernatant liquid were noted. The difference between the initial (pH_0) and final pH (pH_f) values ($\text{pH}_0 - \text{pH}_f$) was plotted against the pH. The point of intersection of the resulting curve at which pH gave the pH_{PZC} . The procedure was repeated for different concentrations of KNO_3 .

2.3. Adsorption experiments

All batch experiments were carried out in 50 mL of an initial dye concentration (C_0) of 2000 mg/L (pH_0 6.5) with 50 mg of adsorbent

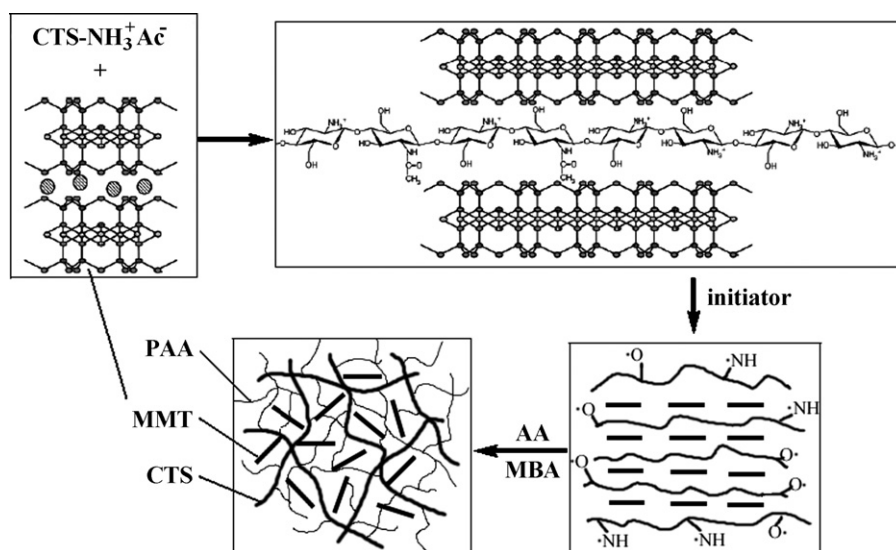


Fig. 2. Schematic process for synthesis of CTS-g-PAA/MMT nanocomposite via in situ intercalated polymerization.

at 30 °C for 120 min and performed on a thermostated shaker (THZ-98A) with a shaking of 120 rpm. The influence of pH was studied by adjusting MB solutions (C_0 , 2000 mg/L) to different pH_0 values (2.0, 3.0, 4.0, 5.0, 6.0, 7.0, 8.0 and 9.0) with 0.1 mol/L NaOH or HCl solution using a pH meter (DELTA-320). For kinetic study, 2000 mg/L dye solutions (50 mL, pH_0 6.5) were agitated with 50 mg of adsorbent at 30 °C for predetermined intervals of time. Batch equilibrium adsorption experiments were carried out by agitating 50 mL of various dye concentrations of MB solution at pH_0 6.5 with 50 mg of adsorbent at 30 °C until equilibrium was established.

The samples were withdrawn from the shaker at predetermined time intervals and the dye solution was separated from the adsorbent by centrifugation at 4500 rpm for 10 min. The absorbencies of samples were measured using a UV–vis spectrophotometer (Specord 200) at 670 nm corresponding to a maximum absorbency of MB. Then the concentrations of the samples were determined by using a linear regression equation obtained by plotting a calibration curve for dye over a range of concentrations. The amounts of MB adsorbed onto samples were calculated by subtracting the final solution concentration from the initial concentration of dye solutions.

2.4. Desorption studies

For batch desorption study, the adsorbent utilized for the adsorption of C_0 of 2000 mg/L was separated from the dye solution by centrifugation. The dye-loaded adsorbent was washed gently with water to remove any unadsorbed dye. Then the spent adsorbent was stirred using a magnetic stirrer with 50 mL of distilled water at different pHs for 120 min, one by one. The desorbed dye was determined as mentioned before.

3. Results and discussion

3.1. Effect of pH value on adsorption

To understand the adsorption mechanism, it is necessary to determine the point of zero charge (pH_{PZC}) of the adsorbent [25]. Adsorption of cations is favored at $pH > pH_{PZC}$, while the adsorption of anions is favored at $pH < pH_{PZC}$. The specific adsorption of cations shifts pH_{PZC} towards lower values, whereas the specific adsorption of anions shifts pH_{PZC} towards higher values. Fig. 3 shows that for all the concentrations of KNO_3 , the zero value of pH lies at the pH_0 value of 6.5, which is considered as the pH_{PZC} of the CTS-g-PAA/MMT nanocomposite.

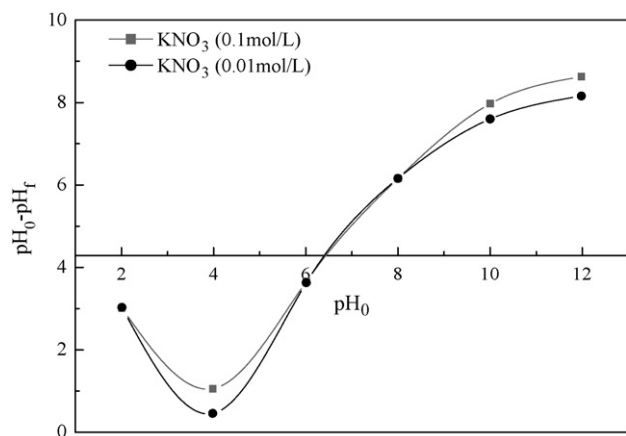


Fig. 3. Point of zero charge of CTS-g-PAA/MMT nanocomposite.

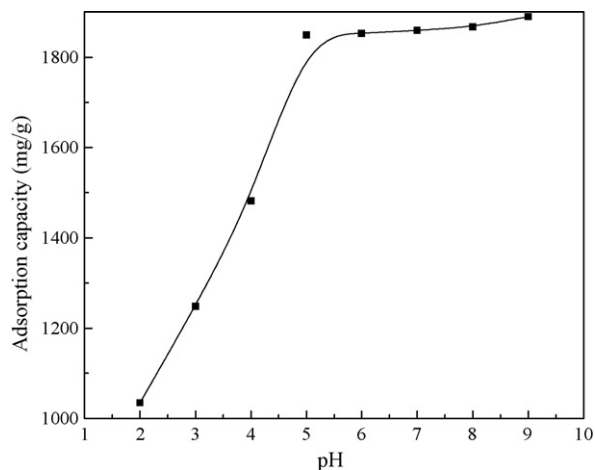


Fig. 4. Effect of the pH values on adsorption capacity of CTS-g-PAA/MMT nanocomposite for MB. Adsorption experiments— C_0 : 2000 mg/L, adsorbent dose (m): 50 mg/50 mL, T : 30 °C, equilibrium time (t): 120 min, wr of AA to CTS: 7.2 and wt%: 30%.

Generally, the adsorption capacity of adsorbent is highly dependent on the pH of the solution. Fig. 4 indicates the effect of the pH value of the initial dye solution on the adsorption capacity of MB on CTS-g-PAA/MMT nanocomposite for C_0 : 2000 mg/L, adsorbent dose (m): 50 mg/50 mL, T : 30 °C, equilibrium time (t): 120 min, wr of AA to CTS: 7.2 and wt%: 30%. As shown in Fig. 4, with the pH value of the solution increased from 2.0 to 5.0, the adsorption capacity increased sharply from 1035 mg/g to 1849 mg/g for the nanocomposite, and then increased continuously from 1849 mg/g to 1890 mg/g with the increase of the pH from 5.0 to 9.0. The increasing tendency of adsorption capacity with increasing the pH value may be attributed to the following facts. At higher pH, most of the carboxylic groups in superadsorbent nanocomposite are ionized and interacted with the dye molecules, which result in an increase of the absorption for MB. In addition, at higher pH, the $-COOH$ groups present in acrylate dissociate to form COO^- , increasing the number of fixed ionized groups. This generates electrostatic repulsion forces among the adjacent ionized groups of polymer networks, inducing an expansion of the polymer chains within the superadsorbent nanocomposite structure, which also result in an increase of the absorption for MB. Similar result has been reported for the adsorption of MB by superadsorbent hydrogel

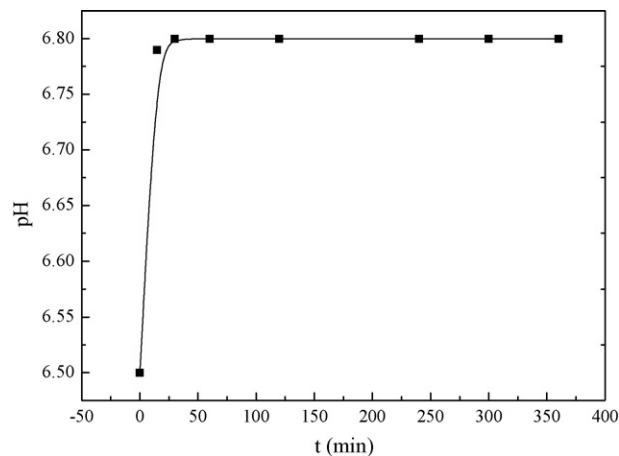


Fig. 5. Variation of pH with time for adsorption capacity of CTS-g-PAA/MMT nanocomposite. Adsorption experiments—dye concentration (C_0): 2000 mg/L, m : 50 mg/50 mL, pH_0 : 6.5, T : 30 °C, wr of AA to CTS: 7.2 and wt%: 30%.

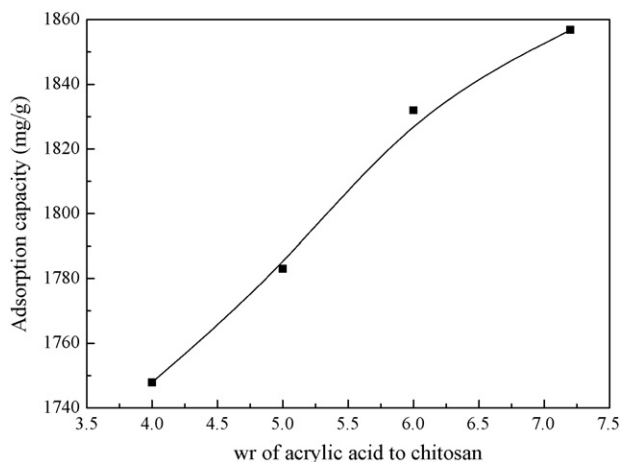


Fig. 6. Effect of weight ratio of AA to CTS on adsorption capacities of CTS-g-PAA/MMT nanocomposites for MB. Adsorption experiments— C_0 : 2000 mg/L, m : 50 mg/50 mL, pH_0 : 6.5, T : 30 °C, t : 120 min and wt%: 30%.

formed by modified gum arabic, polyacrylate and polyacrylamide [22].

Fig. 5 shows variation of pH with time for adsorption capacity of CTS-g-PAA/MMT nanocomposite for C_0 : 2000 mg/L, m : 50 mg/50 mL, pH_0 : 6.5, T : 30 °C, wr of AA to CTS: 7.2 and wt%: 30%. It is found that the system pH changes swiftly during the initial 15 min and, thereafter, the change is gradual. After about 30 min, pH remains almost invariant with time. Maximum pH change is found for MB: pH increases from 6.5 to about 6.8. The extent of pH change during sorption process may not affect the sorption equilibrium and kinetics significantly [26]. Therefore, further studies on adsorptive removal of dyes by CTS-g-PAA/MMT nanocomposite were carried out at a pH 6.5.

3.2. Effect of weight ratio (wr) of AA to CTS on adsorption

The effect of wr of AA to CTS on adsorption capacities of CTS-g-PAA/MMT nanocomposites for MB was investigated and the results are shown in Fig. 6 for C_0 : 2000 mg/L, m : 50 mg/50 mL, pH_0 : 6.5, T : 30 °C, t : 120 min and wt%: 30%. Apparently, the adsorption capacities of the nanocomposites increase continuously with increasing wr of AA to CTS. This observation may be interpreted as follows: on the one hand, more AA molecules could be available in the near of the chain propagating sites of CTS macroradicals with increasing wr of AA to CTS, which enhances the amounts of -COOH groups and then the adsorption capacity is improved. On the other hand, more Na^+ ions are generated in the polymeric network owing to the neutralization of grafted PAA in the nanocomposite. Consequently, the osmotic pressure difference between polymeric network and external dye solution increased, which also results in the higher adsorption capacity of CTS-g-PAA/MMT nanocomposite. Based on the mentioned above, the wr of AA to CTS of 7.2:1 is chosen in this study.

3.3. Effect of MMT content (wt%) on adsorption

Fig. 7 shows the effect of wt% on adsorption capacities of CTS-g-PAA/MMT nanocomposites for MB for C_0 : 2000 mg/L, m : 50 mg/50 mL, pH_0 : 6.5, T : 30 °C, t : 120 min, wr of AA to CTS: 7.2. It is clear that wt% is an important factor affecting adsorption capacity of the nanocomposite. As can be seen from Fig. 7, the adsorption capacity of the nanocomposite increased from 1870 mg/g to 1910 mg/g, as wt% of 2% was introduced. According to the IR analysis and the XRD patterns of MMT and CTS-g-PAA/MMT

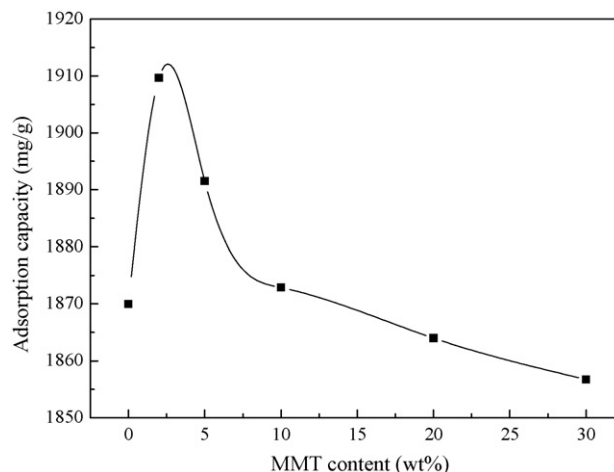


Fig. 7. Effect of MMT content on adsorption capacities of CTS-g-PAA/MMT nanocomposites for MB. Adsorption experiments— C_0 : 2000 mg/L, m : 50 mg/50 mL, pH_0 : 6.5, T : 30 °C, t : 120 min and wr of AA to CTS: 7.2.

[23], -OH of MMT participated in the graft-polymerization and the formation of the exfoliated nanostructure in CTS-g-PAA/MMT, which may improve the polymeric network, and then enhance the adsorption capacity. CTS-g-PAA has tight surface, whereas, the introduced MMT generated a loose and porous surface [23]. This surface is convenient for the penetration of dye molecules into the polymeric network, and then may be of benefit to adsorption capacities of the nanocomposites. However, the adsorption capacities of the nanocomposites decrease with further increasing wt%. The lower tendency of the adsorption capacity with increasing wt% may be attributed to the following facts. The interaction among MMT, CTS and AA became intensive gradually with increasing wt%. Consequently, more chemical and physical crosslinkages were formed in the polymeric network, and then elasticity of the polymer chains decreases, which decreased adsorption capacity of the nanocomposite. Nevertheless, the adsorption capacity of the nanocomposite with wt% of 30% (1857 mg/g) was little decreasing than that of the nanocomposite with wt% of 2% (1910 mg/g). In addition, the cost of MMT is lower than CTS and AA. Therefore, considering the economic advantage, the following discussion will be focused on CTS-g-PAA/MMT nanocomposite with wt% of 30% in this study.

3.4. Effect of temperature (T) on adsorption

The relationship between the temperature and the adsorption capacity of MB by the nanocomposite has been studied in the text for C_0 : 2000 mg/L, m : 50 mg/50 mL, pH_0 : 6.5, t : 120 min, wr of AA to CTS: 7.2 and wt%: 30%. The results show that the adsorption capacity of the nanocomposite increased from 1857 mg/g to 1936 mg/g with increasing T from 30 °C to 40 °C, and then decreased from 1936 mg/g to 1909 mg/g with further increase in T from 40 °C to 50 °C. It is well known that increasing temperature may produce a swelling effect within the internal structure of adsorbent, penetrating the large dye molecule further [27]. However, the mobility of the large dye ions increases with increasing temperature, which leads to a decrease in the adsorption capacity of nanocomposite with further increasing temperature.

3.5. Adsorption kinetics

Fig. 8 shows the effect of contact time on the adsorption capacity of MB by the nanocomposite for C_0 : 2000 mg/L, m : 50 mg/50 mL,

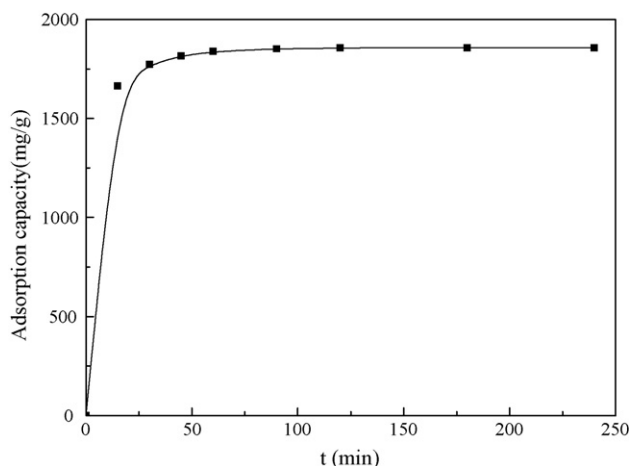


Fig. 8. Effect of the adsorption time on adsorption capacity of CTS-g-PAA/MMT nanocomposite for MB. Adsorption experiments— C_0 : 2000 mg/L, m : 50 mg/50 mL, pH_0 : 6.5, T : 30 °C, wr of AA to CTS: 7.2 and wt%: 30%.

pH_0 : 6.5, T : 30 °C, wr of AA to CTS: 7.2 and wt%: 30%. It can be seen from Fig. 8 that the adsorption capacity of the nanocomposite increased rapidly within 60 min and then changed very little and no further adsorption occurred after 120 min. Therefore, under our experimental conditions, the equilibrium time (t) for the adsorption of MB on the nanocomposite is 120 min.

The pseudo-first-order kinetic model is valid only for the initial adsorption period [25,28]. Therefore, in order to find out the potential rate-controlling steps involved in the adsorption processes of MB onto CTS-g-PAA/MMT nanocomposite, pseudo-second-order kinetic model were used to fit the experimental data.

The pseudo-second-order rate equation is given as [29]:

$$\frac{t}{q_t} = \frac{1}{kq_e^2} + \frac{t}{q_e} \quad (1)$$

where q_e and q_t are the amounts of adsorption dye (mg/g) at equilibrium and at time t (min) and k (g/(mg min)) is the adsorption rate constant of pseudo-second-order adsorption rate.

The initial sorption rate, h (mg/(g min)), as $t \rightarrow 0$ can be defined as

$$h = kq_e^2 \quad (2)$$

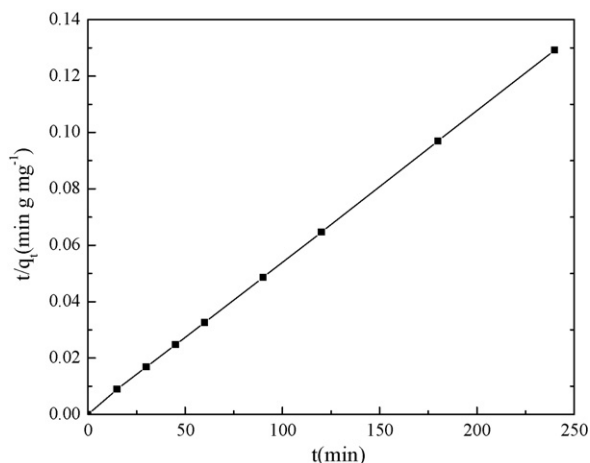


Fig. 9. Pseudo-second-order model for the adsorption of MB by CTS-g-PAA/MMT nanocomposite.

Fig. 9 shows the plot of t/q_t versus t . The value of q_e is obtained from the slope of the plot and h is obtained from the intercept. Since q_e is known from the slope, k can be determined from the value of the initial sorption rate. The experimental data have been analyzed by two correlation coefficients. The linear R^2 coefficient (the coefficient of determination) compares the estimated and actual y-axis values, and ranges in value from 0 to 1 when two arrays of data are fitted to linear equation. If it is 1, there is a perfect correlation in the sample—there is no difference between the estimated and the actual y-axis value. At the other extreme, if the coefficient of determination is 0, the regression equation is not helpful in predicting a y-axis value. The non-linear R^2 -value is based on the actual deviation between the experimental data and the theoretically predicted data and is a better correlation of the experimental data with the equation [25].

The experimental q_e value ($q_{e,exp}$), calculated q_e value ($q_{e,cal}$), k and h along with calculated correlation coefficients, both linear and non-linear for pseudo-second-order model for dyes adsorption are 1857 mg/g, 1871 mg/g, 3.874×10^{-4} g/(mg min), 1356 mg/(g min), 0.9999 and 0.9999, respectively. It can be seen from mentioned above that the $q_{e,exp}$ and the $q_{e,cal}$ values from pseudo-second-order kinetics model are very close to each other. In addition, the calculated correlation coefficients are also very close to each other. These results indicated that the adsorption of MB on superadsorbent nanocomposite followed the pseudo-second-order.

3.6. Adsorption isotherms

The influence of C_0 on adsorption capacities of MB for the nanocomposite is shown in Fig. 10 for m : 50 mg/50 mL, pH_0 : 6.5, T : 30 °C, t : 120 min, wr of AA to CTS: 7.2 and wt%: 30%. It is clear that the C_0 plays an important role in the adsorption capacity of dye onto adsorbent. The results showed that the adsorption capacity of the nanocomposite increased sharply from 1796 mg/g to 1857 mg/g with the C_0 of dye increasing from 1800 mg/L to 2000 mg/L. However, the adsorption capacity of the nanocomposite hardly increased with further increasing the C_0 of dye. This result may be attributed to the fact that the aggregation of MB dye molecules makes it almost impossible for them to diffuse deeper into CTS-g-PAA/MMT nanocomposite structure [9,25,30].

Adsorptions isotherms are important for the description of how molecules of adsorbate interact with adsorbent surface. Hence, the correlation of equilibrium data using either a theoretical or

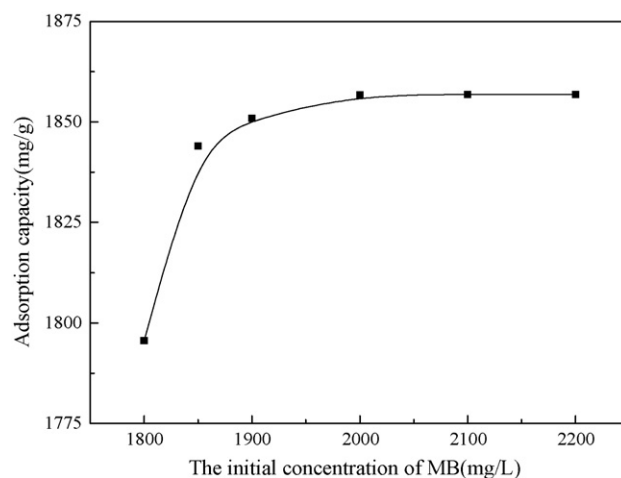


Fig. 10. Effect of the dye concentration on adsorption capacity of CTS-g-PAA/MMT nanocomposite for MB. Adsorption experiments— m : 50 mg/50 mL, pH_0 : 6.5, T : 30 °C, t : 120 min, wr of AA to CTS: 7.2 and wt%: 30%.

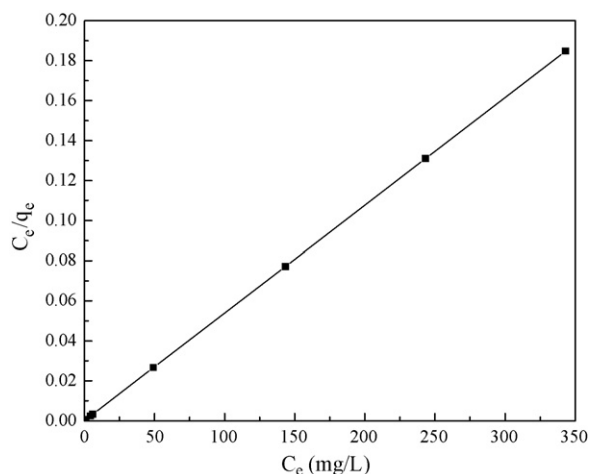


Fig. 11. Langmuir plot for the adsorption of MB by CTS-g-PAA/MMT nanocomposite.

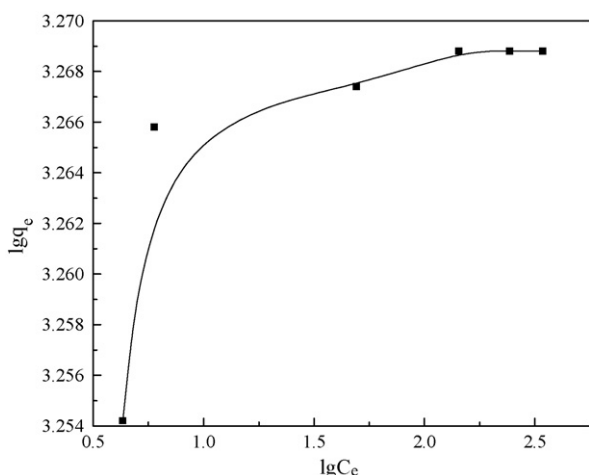


Fig. 12. Freundlich plot for the adsorption of MB by CTS-g-PAA/MMT nanocomposite.

empirical equation is essential for the adsorption interpretation and prediction of the extent of adsorption [31]. The equilibrium adsorption data were generally interpreted using Langmuir and Freundlich [32], which are represented by the following equations, respectively:

$$\frac{C_e}{q_e} = \frac{1}{bq_m} + \frac{C_e}{q_m} \quad (3)$$

$$q_e = K_f C_e^{1/n} \quad (4)$$

where q_m (mg/g) and b (L/mg) are Langmuir isotherm coefficients. The value of q_m represents the maximum adsorption capacity. K_f (mg/g) and n are Freundlich constants. Two adsorption isotherms were constructed by plotting C_e/q_e versus C_e and $\log q_e$ versus $\log C_e$.

Table 1

The q_m values for the adsorption of MB on different adsorbents

Adsorbents	C_0 (mg/L)	pH ₀	m (mg)	C_0/m	q_m (mg/g)	Reference
CTS-g-PAA/MMT	2000	6.5	50	40	1859	Our data in the paper
MMT	200	–	100	2	322.6	[19]
Clay	100	5.65	100	1	58.2	[20]
SH	50	8	50	1	48	[22]

C_0 : the initial MB concentration; pH₀: the initial MB pH; m : adsorbent dose; C_0/m : initial concentration/adsorbent dosage ratio; SH: superabsorbent hydrogel formed by modified gum arabic, polyacrylate and polyacrylamide.

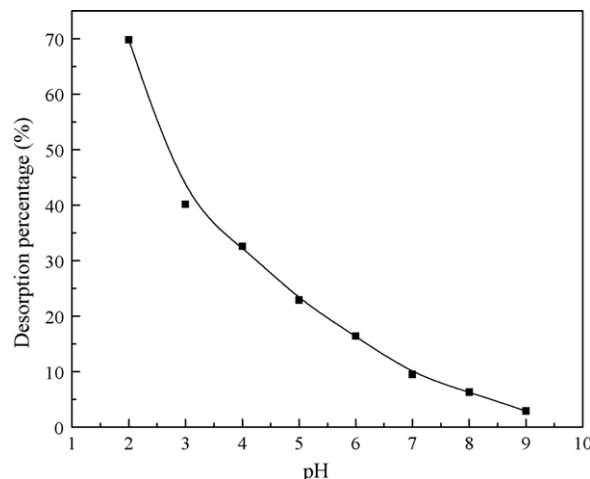


Fig. 13. Effect of pH on desorption percentage of dye from dye-loaded CTS-g-PAA/MMT nanocomposite. Adsorption experiments— C_0 : 2000 mg/L, m : 50 mg/50 mL, pH₀: 6.5, T : 30 °C, t : 120 min, wr of AA to CTS: 7.2 and wt%: 30%.

Figs. 11 and 12 show the plot of C_e/q_e versus C_e and $\log q_e$ versus $\log C_e$, respectively. Constant b of Langmuir model is 0.9993 L/mg. Constants K_f and $1/n$ of Freundlich model are 1.805×10^3 (mg/g)/(mg/L)^{1/n} and 5.430×10^{-3} , respectively. The correlation coefficients (R^2) of Langmuir and Freundlich models are 1 and 0.7780 for the nanocomposite, respectively. In addition, the q_m value for the adsorption of MB by the nanocomposite was 1859 mg/g, which are same as the experiment data 1857 mg/g for the nanocomposite. Obviously, the Langmuir isotherm, compared with the Freundlich isotherm, describes the adsorption of MB on the nanocomposite very well. This means the monolayer coverage of the dye on the surface of the nanocomposite. Similar behavior was also found for the adsorption of MB onto precursor and quaternary ammonium compounds-modified montmorillonite [19], clay [21] and Cu(II)-exchanged montmorillonite [33]. The q_m value for the adsorption of MB on CTS-g-PAA/MMT nanocomposite was compared with those of other adsorbents (see Table 1). It can be seen from Table 1 that the q_m value of CTS-g-PAA/MMT was much higher than those of other adsorbents such as MMT, clay, SH and so on. Therefore, CTS-g-PAA/MMT nanocomposite can be very effectively used as an adsorbent in treatment of MB dye wastewaters.

3.7. Desorption of MB

Desorption studies can help elucidating the mechanism of an adsorption process. If the dye adsorbed onto the adsorbent can be desorbed by water, it can be said that the attachment of the dye onto the adsorbent is by weak bonds. If the strong acids, such as HCl can desorb the dye, it can be said that the attachment of the dye onto the adsorbent is by ion exchange or electrostatic attraction [25]. Hence, distilled water of different pHs was used in the elution of dyes from the nanocomposite. Effect of pH on desorption per-

centage of dye from dye-loaded CTS-g-PAA/MMT nanocomposite is shown in Fig. 13 for C_0 : 2000 mg/L, m : 50 mg/50 mL, pH_0 : 6.5, T : 30 °C, t : 120 min, wr of AA to CTS: 7.2 and wt%: 30%. Apparently, the desorption percentage of the nanocomposite decreased sharply with increasing the pH of distilled water. Low desorption was obtained with pH 9.0 and the percentage of desorption for the nanocomposite was only 2.9%, while in the case of pH 2.0, 69.8% was obtained. The fact that the high desorption occurred with pH 2.0 suggested that adsorption of MB onto the nanocomposite carried out significantly via electrostatic attraction, which further substantiated the discussion of the effect of pH value on adsorption. These results indicated that the nanocomposite provided the potential for regeneration and reuse after MB dye adsorption despite 30% dye remaining in the adsorbent in the case of pH 2.0. In addition, on one hand, spent CTS-g-PAA/MMT nanocomposite can be used as craftwork rockcrystal. On the other hand, spent CTS-g-PAA/MMT nanocomposite also can be used as a fuel due to its high-polymer content and the bottom ash after its combustion/incineration can be blended with clay/cement–concrete mixture to make bricks and building blocks for its safe disposal. So, the nanocomposite can be used as an alternative-adsorbing agent in dye wastewaters.

4. Conclusion

The introduced MMT could generate a loose and porous surface that is of benefit to adsorption ability of the nanocomposite. The pH_{PZC} was found to be 6.5. Results obtained from this study showed that the adsorption capacity of the nanocomposite for MB increased with increasing pH_0 . The wr of AA to CTS and wt% have great influence on adsorption capacities of the nanocomposites. Introducing a small amount of MMT could improve adsorption ability of the CTS-g-PAA superadsorbent. Kinetic data of adsorption were well fitted by the pseudo-second-order kinetic model. The equilibrium experimental data fit perfectly with the Langmuir isotherm. It implies the monolayer formation of the surface on the nanocomposite by MB molecules. The maximum adsorption capacity was 1859 mg/g for CTS-g-PAA/MMT with wr of AA to CTS of 7.2:1 and wt% of 30%. In desorption studies, comparatively high desorption of dyes were obtained with pH 2.0 of distilled water. This indicates that the nanocomposite provided the potential for regeneration and reuse after MB dye adsorption. As a result, it can be said that the CTS-g-PAA/MMT nanocomposite is a very effective adsorbent for the removal of MB from aqueous solution.

Acknowledgement

This work was financially supported by the science and technology major project of Jiangsu Province, PR China (no. BS2007118).

References

- [1] M.S. Chiou, P. Ho, Y. Ho, H.Y. Li, *Dyes Pigments* 60 (2004) 69–84.
- [2] R. Gong, Y. Ding, M. Li, C. Yang, H. Liu, Y. Sun, *Dyes Pigments* 64 (2005) 187–192.
- [3] S. Seshadri, P.L. Bishop, A.M. Agha, *Waste Manage.* 15 (1994) 127–137.
- [4] J. Panswed, S. Wongchaisuwan, *Water Sci. Technol.* 18 (1986) 139–144.
- [5] G. Ciardelli, L. Corsi, M. Marucci, *Conserv. Recycl.* 31 (2000) 189–197.
- [6] K. Swaminathan, S. Sandhya, A. Carmalin Sophia, K. Pachhade, Y.V. Subrahmanyam, *Chemosphere* 50 (2003) 619–625.
- [7] M. Muthukumar, N. Selvakumar, *Dyes Pigments* 62 (2004) 221–228.
- [8] A. Alinsafi, M. Khemis, M.N. Pons, J.P. Leclerc, A. Yaacoubi, A. Benhammou, A. Nejmeddine, *Chem. Eng. Process.* 44 (2005) 461–470.
- [9] I.D. Mall, V.C. Srivastava, N.K. Agarwal, I.M. Mishra, *Chemosphere* 61 (2005) 492–501.
- [10] M.Y. Chang, R.S. Juang, *J. Colloid Interf. Sci.* 278 (2004) 18–25.
- [11] R.S. Vieira, M.M. Beppu, *Colloids Surf. A: Physicochem. Eng. Aspects* 279 (2006) 196–207.
- [12] R.S. Juang, C.Y. Ju, *Ind. Eng. Chem. Res.* 36 (1997) 5403–5409.
- [13] G. Crini, *Bioresour. Technol.* 97 (2006) 1061–1085.
- [14] R.A. Shawabkeh, M.F. Tutunji, *Appl. Clay Sci.* 24 (2003) 111–120.
- [15] M.G. Neumann, F. Gessner, C.C. Schmitt, R. Sartori, *J. Colloid Interf. Sci.* 255 (2002) 254–259.
- [16] A.H. Gemeay, A.S. El-Sherbiny, A.B. Zaki, *J. Colloid Interf. Sci.* 245 (2002) 116–125.
- [17] N. Miyamoto, R. Kawai, K. Kuroda, M. Ogawa, *Appl. Clay Sci.* 16 (2000) 161–170.
- [18] A.H. Gemeay, *J. Colloid Interf. Sci.* 251 (2002) 235–241.
- [19] R. Wibulswas, *Sep. Purif. Technol.* 39 (2004) 3–12.
- [20] A. Gürses, Ç. Doğar, M. Yalçın, M. Açıkyıldız, R. Bayrak, S. Karaca, *J. Hazard. Mater.* 31 (2006) 217–228.
- [21] A. Gürses, S. Karaca, Ç. Doğar, R. Bayrak, M. Açıkyıldız, M. Yalçın, *J. Colloid Interf. Sci.* 269 (2004) 310–314.
- [22] A.T. Paulino, M.R. Guilherme, A.V. Reis, G.M. Campese, E.C. Muniz, J. Nozaki, *J. Colloid Interf. Sci.* 301 (2006) 55–62.
- [23] J.P. Zhang, L. Wang, A.Q. Wang, *Ind. Eng. Chem. Res.* 46 (2007) 2497–2502.
- [24] L.S. Balistreri, J.W. Murray, *Am. J. Sci.* 281 (1981) 788–806.
- [25] I.D. Mall, V.C. Srivastava, G.V.A. Kumar, I.M. Mishra, *Colloids Surf. A: Physicochem. Eng. Aspects* 278 (2006) 175–187.
- [26] C. Tien, *Sep. Purif. Technol.* 54 (2007) 277–278.
- [27] K.G. Bhattacharyya, A. Sarma, *Dyes Pigments* 57 (2003) 211–222.
- [28] V.C. Srivastava, M.M. Swamy, I.D. Mall, B. Prasad, I.M. Mishra, *Colloids Surf. A: Physicochem. Eng. Aspects* 272 (2006) 89–104.
- [29] Y.S. Ho, G. McKay, *Process Biochem.* 34 (1999) 451–465.
- [30] E. Coates, *J. Soc. Dyers Colour.* 85 (1969) 355–368.
- [31] E.L. Grabowska, G. Gryglewicz, *Dyes Pigments* 74 (2007) 34–40.
- [32] K. Periasamy, C. Namasivayam, *Waste Manage.* 15 (1995) 63–68.
- [33] Y.L. Ma, Z.R. Xu, T. Guo, P. You, *J. Colloid Interf. Sci.* 280 (2004) 283–288.